A. Boev, R. Bregović, and A. Gotchev, “Design of tunable anti-aliasing filters for multiview displays,” *Proc. SPIE-IS&T Stereoscopic displays and applications XXII*, San Francisco, USA, Jan. 2011, doi:10.1117/12.873465, 12 pages.

Design of tuneable anti-aliasing filters for multiview displays

Atanas Boev, Robert Bregovic, Atanas Gotchev
Institute of Signal Processing, Tampere University of Technology, P.O.Box 553, 33101 Tampere, Finland

ABSTRACT

Multiview displays suffer from two common artifacts – Moiré, caused by aliasing, and ghosting artifacts caused by crosstalk. By measuring the angular brightness function of each TFT element we create so-called brightness mask, which allows us to simulate the display output for a given input image. We consider multiview display as image processing channel and model the artifacts as distortions of the input signal. We test the channel by using a set of signals with various frequency components as input, and analyzing the output in the frequency domain. We derive the so-called bandpass region of the display, where the distortions introduced to the input signals are under certain threshold. Then, we extend the simulations including input signals with varying disparity, and obtain multiple passbands – one for each disparity level. We approximate each passband with a rectangle and store the height and width of that rectangle in a table.

We propose an artifact mitigation framework which can be used for realtime processing of textures with known apparent depth. The framework gives the user ability to set so-called “3D-shapness” – a parameter, which controls the trade-off between visibility of details and presence of artifacts. The “3D-sharpness parameter determines what level of distortions is allowed in the final image, regardless of its disparity. The framework uses the approximated width and height of the passband areas in order to design an optimal (for the needed disparity and desired distortion level) anti-aliasing filter. We discuss a methodology for filter design, and show example results, based on measurements of an 8-view display.

Keywords: multiview displays, anti-aliasing filters, optical measurements, Moiré, ghosting artifacts, filter design, 3D-sharpness

1. INTRODUCTION

Multiview displays can create stereoscopic 3D effect without requiring the observer to wear specially designed glasses. They work by simultaneously visualizing a number of images, each one visible at different angle. Most often, a multiview display uses a TFT-LCD matrix for image creation, and an additional *optical layer* mounted on top, which redirects the light created by the TFT elements [1,2]. The visibility of the TFT color components (also known as *subpixels*) becomes a function of the observation angle. From each angle, a group of subpixels is predominantly visible, and forms an image. Such image is called a *view*. If multiple observations of the same scene are properly assigned to the views of a multiview display, the stereoscopic 3D effect is created. The process of mapping multiple images to the subpixels of a multiview display is known as *interleaving*, and the map, which defines the correspondence between subpixels and view number is known as *interleaving map*. The interleaving map has the full resolution of the TFT-LCD matrix of the display, but most often it can be fully described by a smaller repetitive structure that we refer to as *interleaving pattern*.

The design of the optical filter involves a trade-off between number of views, resolution of a view and the quality of view reconstruction. Multiview displays are susceptible to a number of visual artifacts [3], but two are the most pronounced – Moiré and ghosting [3,4,5]. Mapping an image to the visible pixels of a view involves subsampling, which often happens on a non-rectangular grid. Failing to properly pre-filter the image creates aliasing, which manifests itself as Moiré artifacts. The effect is more complicated for objects with pronounced depth. In that case, observations of the same object appear in different horizontal position in each view. The horizontal offset between the observations is known as *disparity*. The disparity between the observations in different views creates the stereoscopic illusion of depth. In this work, we refer to the illusory distance to the object created by the stereoscopic effect as *apparent depth*. Positive disparity creates apparent depth behind the screen plane, and negative disparity creates apparent depth in front of the screen. In order to avoid banding and image flipping artifacts, the observation zones of the views are interspersed, and from each observation direction a number of views are simultaneously visible (albeit with different brightness). This effect is modeled as crosstalk between the views. The combination of crosstalk and disparity creates horizontally shifted, semi-visible replica of visualized object – an effect called *ghost images*, or ghosting.

Moiré artifacts are especially visible in images with high contrast and sharp details – such as text or GUI widgets. In 3D scenes, such content can have different apparent depth, for example depth of subtitles is rendered according to depth of the rest of the scene. The visibility of distortions varies with the frequency, orientation, and depth of the content. In previous work, we proposed a methodology for design of anti-aliasing filters based on the frequency performance of a multiview display 6. These filters were optimal for 2D content with no apparent depth. Additionally, we have found that the filter that fully suppresses aliasing does not always give the best perceptual quality 7. Some people prefer sharper-looking images at the expense of some Moiré artifacts. In this work, we extend our methodology towards design of anti-aliasing filters for content at different disparity levels. We discuss methodology for design of tuneable filters, which depend on two parameters – apparent depth and desired sharpness. The sharpness parameter is expressed in terms of signal-to-distortion ratio, which we claim to affect the visibility of aliasing in perceptually linear fashion, regardless of the apparent depth. Throughout the paper, we give measurement results for an 8-view multiview display as a practical example. The display we use for the examples is 23"-Multiview Display AD, produced by Opticality (formely X3D Corporation) to which we refer to as the *X3D-display* 8.

The paper is structured as follows. In the next section, we introduce the method for performance analysis in the frequency domain, which is used for obtaining the so-called passband region of the display. In Section 3 we study the passband region for input signals with varying apparent depth. In Section 4 we introduce the concept of perceived distortion, and show how to derive the passband region as a function of the distortion percentage. Then, in Section 5 we propose a combination of display measurements and image processing framework, that uses tunable filters for anti-aliasing of objects with given depth for desired sharpness for a given multiview display. Section 6 explains the design of the tunable filters used in this paper. Finally, in Section 7 we give examples for the performance of the filter, optimized for the X3D-display.

2. ESTIMATING THE DISPLAY PERFORMANCE IN THE FREQUENCY DOMAIN

2.1 Multiview display as image processing channel

Most often, the optical layer has a regular structure, and affects the underlying image in a non-uniform way. Therefore image details with certain density and orientation are more prone to distortion than others [12]. Notable exception are displays with random hole distribution 9 where all textures would be distorted equally despite of their frequency content. In order to study how various frequency components get deteriorated by Moiré and ghosting artifacts, we propose a model of a multiview display that considers the display as an image processing channel. The model follows the steps of rendering 2D texture with given apparent depth on a multiview display. Block diagram of the model is shown in Figure 1.

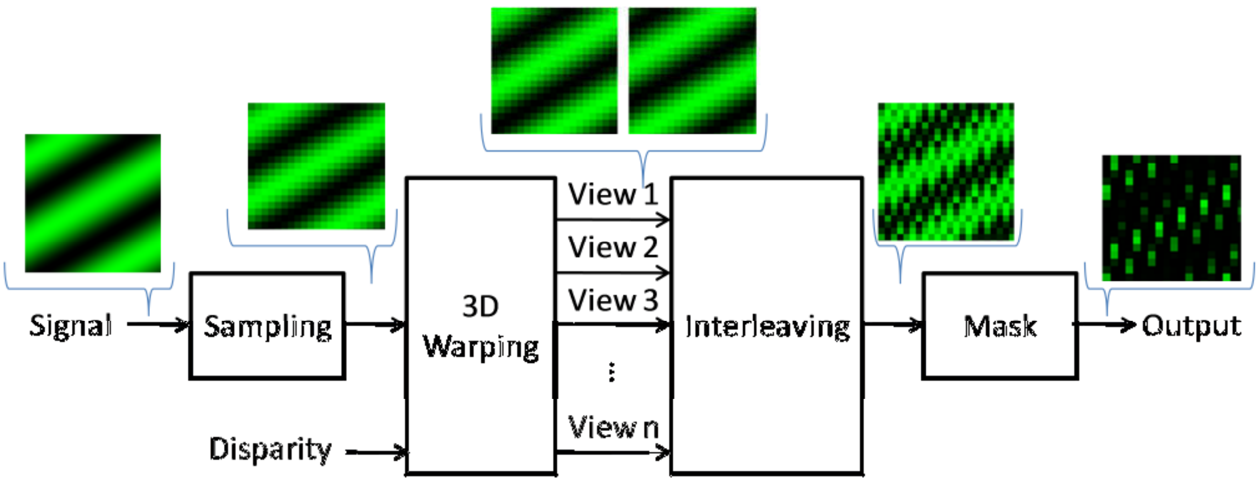

Figure 1, model of a multiview display as image processing channel. The model assumes that the input signal is 2D texture with known apparent depth.

The input to the model is a continuous 2D signal – e.g. text, GUI widget or texture patch. The signal is sampled with the resolution of the underlying TFT-LCD (in other words, with the resolution of the interleaving map). The next step is 3D warping. In order to render the input signal at given apparent depth, shifted versions of the sampled signal are created and assigned to different views. After that, all views are interleaved into one compound image, as it is prescribed by the interleaving map of the multiview display. Since the compound image has the same resolution as the interleaving map, the interleaving process involves downsampling. From each source image only part of the pixels are included in the compound image. The compound image is shown on the TFT-LCD matrix and is transformed by the optical layer. The optical layer acts as a mask, which alters the brightness of each underlying TFT element as a function of the angle. In the ideal case, the visible image should be replica of the image in one of the views. In the real case, parts of the input image are missing, and parts of the images which belong to other views are partially visible.

2.2 Simulation of the display output

The interleaving pattern is provided to the end user, for example the pattern of the X3D-display is seen in Figure 2a. However, such patterns are often imprecise and deriving it experimentally might give more accurate results. In a previous work, we introduced a methodology for deriving the interleaving pattern of a multiview display, and for deriving the so-called angular visibility function of each TFT element of that display [10]. For X3D-display we found 24 distinctive groups of TFT elements with equivalent angular visibility, as opposed to 8 views as stated in the manual. Hence, one can use the X3D-display with 24 views, albeit with low resolution in each view and high crosstalk between the neighboring views.

	Column 1			Column 2			Column 3	
row	1R	1G	1B	2R	2G	2B	3R	3G
1	1	2	3	4	5	6	7	8
2	2	3	4	5	6	7	8	1
3	2	3	4	5	6	7	8	1
4	3	4	5	6	7	8	1	2
5	4	5	6	7	8	1	2	3
6	4	5	6	7	8	1	2	3
7	5	6	7	8	1	2	3	4
8	6	7	8	1	2	3	4	5
9	6	7	8	1	2	3	4	5
10	7	8	1	2	3	4	5	6
11	8	1	2	3	4	5	6	7
12	8	1	2	3	4	5	6	7

a)

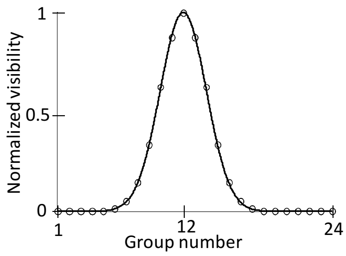

b)

	Column 1			Column 2			Column 3	
row	1R	1G	1B	2R	2G	2B	3R	3G
1	0.1	0.13	0.45	0.74	0.55	0.14	0.1	0.1
2	0.11	0.25	0.73	0.66	0.19	0.11	0.1	0.09
3	0.16	0.65	0.71	0.34	0.12	0.1	0.1	0.1
4	0.45	0.74	0.55	0.14	0.1	0.1	0.1	0.13
5	0.73	0.66	0.19	0.11	0.1	0.09	0.11	0.25
6	0.71	0.34	0.12	0.1	0.1	0.1	0.16	0.65
7	0.55	0.14	0.1	0.1	0.1	0.13	0.45	0.74
8	0.19	0.11	0.1	0.09	0.11	0.25	0.73	0.66
9	0.12	0.1	0.1	0.1	0.16	0.65	0.71	0.34
10	0.1	0.1	0.1	0.13	0.45	0.74	0.55	0.14
11	0.1	0.09	0.11	0.25	0.73	0.66	0.19	0.11
12	0.1	0.1	0.16	0.65	0.71	0.34	0.12	0.1

c)

Figure 2, deriving the visibility mask of X3D-display: a) interleaving pattern, b) measured visibility per group of TFT elements, c) visibility pattern, that can be used as weighting mask for simulating the effect of the optical layer.

One of the commonly measured parameters of a multiview display is the angular brightness of a TFT element, which is the brightness of that element as a function of the observation angle. In this work we use so-called *angular visibility*, which is proportional to the angular brightness, but is normalized in the range between 0 and 1, where 1 is the maximum brightness of a given TFT element. For example, the angular visibility for the 24 groups of TFT elements as seen directly in front of X3D-display is given in Figure 2b. The angular visibility can be directly used as a weighting mask on the values of the interleaved image. This allows the appearance of a multiview display to be simulated for given interleaved image and observation angle. In our experiments, we simulate X3D-display as having 8 views, as given in the display manual, but use the precise weighting mask based on the derived 24 groups of TFT elements with similar angular visibility[10]. The weighting mask is shown in Figure 2c.

a) b) c)

Figure 3, simulation of the display output: a) input signal, b) simulated output, c) photograph input signal, visualized on X3D-display.

In our experiments, we simulate X3D display as it would be seen directly in front of the screen, at 150cm distance, which is the sweet-spot of view number 5. One of our test images can be seen in Figure 3a, and its corresponding simulated version can be seen in Figure 3b. For comparison, in Figure 3c we give photograph of the same image, visualized on the X3D-display.

2.3 Performance analysis

The most important question in connection with a multiview display is related to the proper representation of an image, that is, will an image be properly seen on the display or not? In order to answer this, we must determine which signal frequencies can be properly represented on the screen. In theory, we could use our knowledge about the interleaving pattern and the corresponding brightness (see Figure 2) to derive theoretical expressions that would describe the performance of the display in the frequency domain. Unfortunately, this is a mathematically very demanding task. In order to simplify the analysis, in this paper we will use the method introduced in [10] that was derived for analyzing the display based on a set of images obtained by photographing the display (measurements). From the method point of view, it does not matter if the processed image is a photo of the display or is simulated. Since, we can easily simulate the output of the display, the performance analysis in this paper becomes straightforward. It should be pointed out that the results obtained by simulation and the ones obtained by measurement can considerably differ from each other for a given display due to various effects in the display that are not modeled in the simulation. However, for presenting the basic concept of tunable filters introduced in this paper, simulation results will be sufficient. For completeness of this paper, next, we will briefly describe the method proposed in [10]. More detail about the method can be found there.

In the proposed method all analysis is done in the frequency domain. The method can be summarized by the following five steps. First, we prepare an image having a signal of a given frequency (f_{x_0}, f_{y_0}) with f_{x_0} and f_{y_0} being the frequencies of the input signal in horizontal and vertical direction, respectively. In this paper, all frequencies are normalized to one, with one corresponding to half of the sampling rate. Second, by applying the interleaving pattern and the visibility mask we prepare a simulated image (see Section 2.2). Third, we calculate the spectrum of the simulated image. We normalize the spectrum towards the input signal, that is, the amplitude of the input frequency component is normalized to be zero dB in the evaluated spectrum. Instead of having only peaks at the input signal frequency, due to the interleaving pattern, the spectrum of the simulated image has peaks on multiple places. We have found out that from the visual quality viewpoint, we are only interested in fequency components that have a lower frequency than the input signal [12].This corresponds to frequencies inside a circle with radius

$$r_0 = \sqrt{f_{x_0}^2 + f_{y_0}^2}.$$

Fourth, we apply a threshold criterion on the spectrum. The threshold level depends on the desired distortion. A lower threshold will correspond to tougher requirements on the image, and consequently, on a lower visible image distortion on the display. Fifth, after the threshold is applied, we check if there are any sinusoidal components left inside the circle with radius r_0 beside the DC component. If no, then we conclude that a signal with this particular frequency will be properly represented (visible) on the display. We define that this frequency is in the passband of the display. This is illustrated in Figure 4. As seen in Figure 4c, there are no frequency components above the threshold in the area of interest. Therefore, in Figure 4b we can see the most important features of the input signal. If there are signals present inside the circle with radius r_0, then the image will be represented on the display with distortion higher than desired. Therefore we do not want signals of such frequency in our input signal, that is, we have to filter it out. We will define that this frequency is in the stopband of the display. An example is illustrated in Figure 5. As seen in Figure 5c, there are peaks inside the radius of interest. Therefore, in Figure 5b the input signal is lost

By repeating the above described procedure for images with signals of various frequencies in the intervals $f_x \in [-0, 1]$ and $f_y \in [-1, 1]$, we can determine all frequencies that will be properly represented on the screen, that is, the passband of the display. In the case of the X3D-display we estimate the passband as shown in Figure 6. In the figure, the simulated passband frequencies are marked with dots and the passband edge is emphasized with the blue line. Please note that the passband area presented in this figure (same applies to figures in the following sections) is discrete only due to our discrete simulation. We assume that the passband is continuous and covers all frequencies in the area bordered by the blue line. This figure tells us which frequency can be present in the input image on order for the image to be properly represented on the screen. In this figure, a threshold of 26dB has been used. As described in [10], this threshold has been derived experimentally and it has turned out to be a good choice in practice.

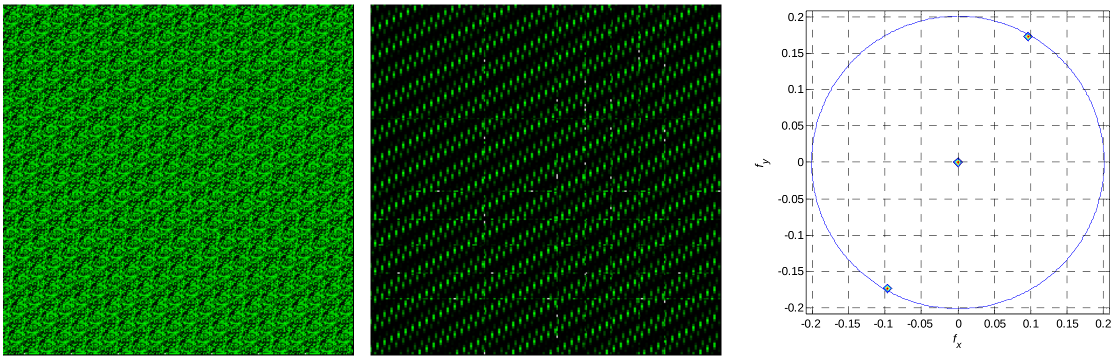

a) b) c)

Figure 4, data analysis for signal $f_x = 0.1$ and $f_y = 0.175$ (signal in the passband): a) input signal, b) simulated output, c) spectrum in the area of interest.

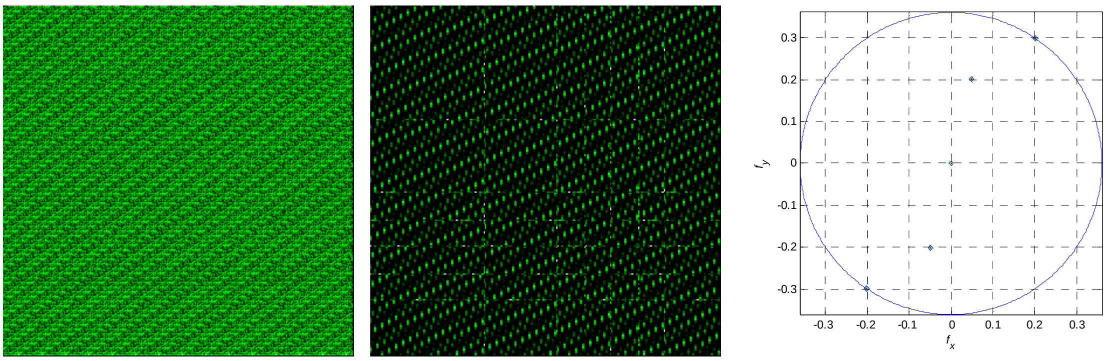

a) b) c)

Figure 5, data analysis for signal $f_x = 0.2$ and $f_y = 0.3$ (signal in the stopband): a) input signal, b) simulated output, c) spectrum in the area of interest.

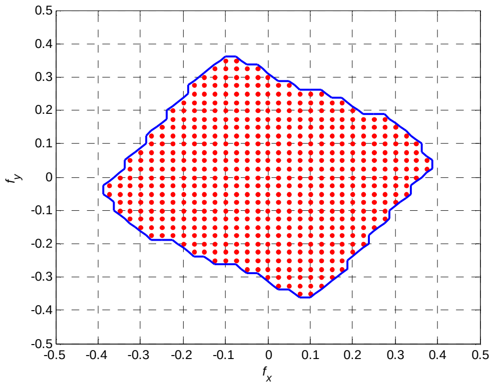

Figure 6, passband for the X3D-display evaluated based on the simulated data for 26dB threshold .

A. Boev, R. Bregović, and A. Gotchev, “Design of tunable anti-aliasing filters for multiview displays,” *Proc. SPIE-IS&T Stereoscopic displays and applications XXII*, San Francisco, USA, Jan. 2011, doi:10.1117/12.873465, 12 pages.

3. FREQUENCY PERFORMANCE VERSUS APPARENT DEPTH

3.1 Rendering objects with apparent depth

In a 3D scene, visualized on a multiview display, all objects are actually projected onto the surface of the display. However, since such display can visualize different images for a number of observation angles, it is possible to create false parallax and illusion of an object appearing in front of, or behind the display surface. Consider the example on Figure 7a. If a real object (e.g. the star-shaped mark on the Figure) appears in front of the display, according to the observation angle its projections appear on different position on the display (as marked with A, B, C, and D on the same Figure). If the multiview display visualizes a scene where the star-shaped object changes its position on the display as a function of the observation angle, this creates the impression of a virtual star-shaped object, hovering at apparent distance l_a in front the display, as exemplified in Figure 7a. This allows for a limited head parallax, where the observer can look at the scene from different angles. Furthermore, as each eye of the observer sees different view, the parallax of the virtual object creates stereoscopic illusion. Since eyes usually appear on horizontal line, and the distance between eyes is constant, the projections of the virtual object appear on equal distances on the screen surface as marked with A, B, C, D in Figure 7a. This corresponds to the constant disparity d in pixels between the observations of the same object in different views. For negative d (horizontal coordinate decreases with view number, as shown in Figure 7b) the object appears behind the surface of the display. For positive d the object appears in front of the display.

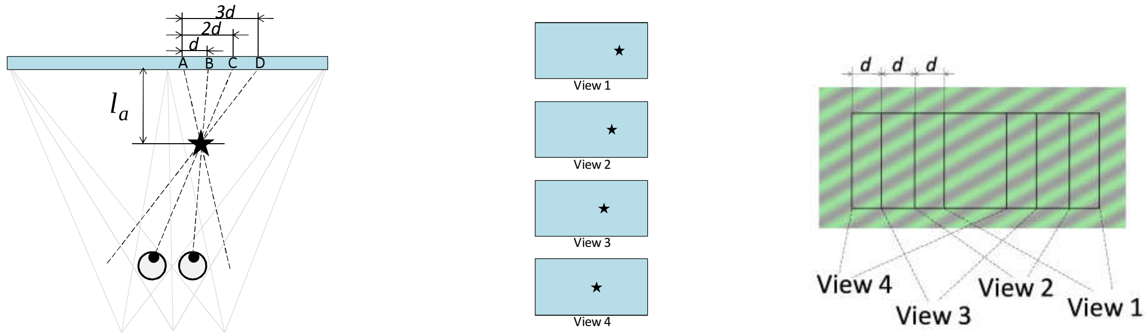

a) b) c)

Figure 7, disparity versus apparent depth: a) projections of a virtual object on the surface of a multiview display, b) position of a virtual object in different views, and c) cropping windows used for creating disparity between views.

3.2 Preparing test images

In order to study the display passband for test signals with different apparent depth, we rendered 2D test signals with different apparent depth. As input, we used test signals with various (known) frequencies (f_x, f_y). From each test signal we prepared a number of interleaved images with different apparent depth following a two step procedure. First, we prepared 8 views from each test image, by cropping the test image at different places as shown in Figure 7c. The cropping window for each view is shifted horizontally with an offset $s_n = d \cdot n$, where s_n is the offset for the n-th view, n is the view number and d is the targeted disparity. Then we interleaved the views into one interleaved test image. By changing the disparity d we simulate the process of putting the test signals at different apparent depths. In our experiments d varies between -10 and 10. To each interleaved test image, we applied the weighting mask which simulates the effect of the optical layer over the visibility of TFT elements. The weighting mask we used is the one derived for the X3D-display, and shown in Figure 2c.

3.3 Performance analysis for varying disparity

We applied the procedure described in Section 2.3 on all simulated images (images with various input frequencies and disparities) generated as described in the previous section. We used the same threshold criteria as earlier, namely, 26dB. In this way we estimated the frequency domain behavior of the display for different disparities. As an example, in Figure 8a and Figure 8b we show the display passband for the X3D-display for disparities 5 and 10, respectively. Based on these figures and Figure 6 it is obvious that different filters are needed for different disparity levels because the display passband has a different shape for different disparities.

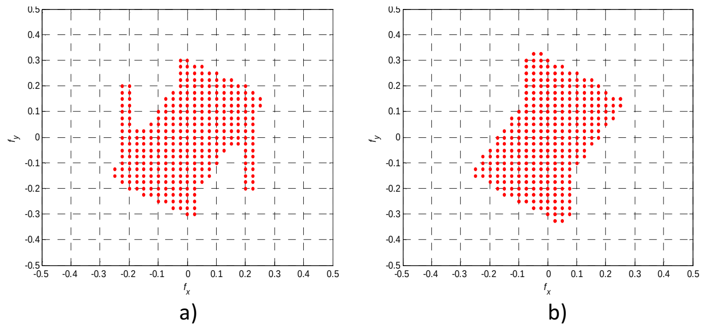

Figure 8, passband of the X3D-display based on simulated data for 26dB threshold and disparity: a) $d = 5$, b) $d = 10$.

4. FREQUENCY PERFORMANCE VERSUS PERCEIVED CROSSTALK

4.1 Perception of crosstalk

Ghosting artifacts are a form of image distortion. An observer labels some of distortion as being ghosting artifacts, if he or she is able to recognize repetitive structures and double contours. However, the human visual system (HVS) is not especially sensitive to ghosting artifacts in comparison to other structural distortions. HVS is optimized for perceiving the structure of the image, and is less sensitive to global contrast or brightness variance [11]. Many visual quality metrics attempt to assess the perceptual difference by estimating structural distortions of the image [12, 13]. The Weber-Fletcher law states that perceptibility of a change in stimuli is proportional to the amplitude of the stimuli. The works that assess visibility of crosstalk in stereoscopic images in typical observation conditions also measure the crosstalk as percentage of the input signal 5. According to 5 the acceptable crosstalk varies between 5% (barely visible) and 30% (barely acceptable). We assume that visibility of image distortion is proportional to the visibility of crosstalk. Therefore, image distortion of 5% would be barely visible, and 30% distortion would be barely acceptable.

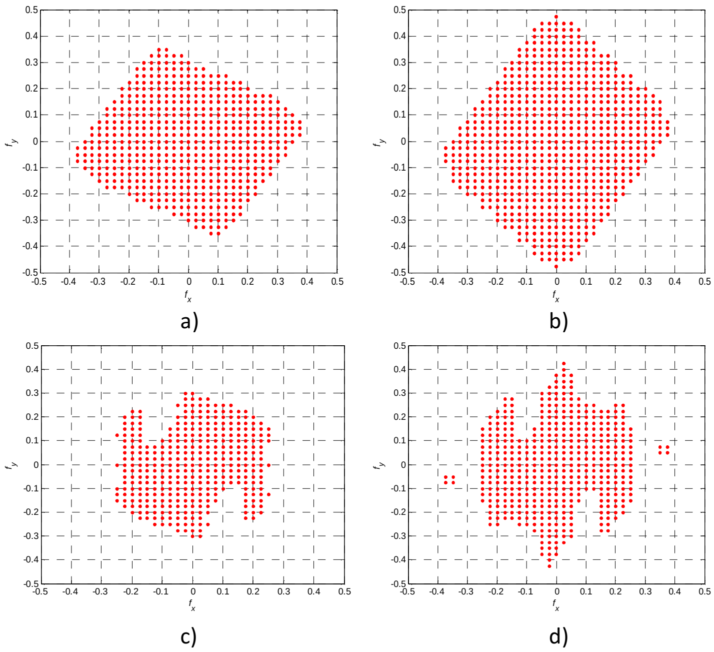

Figure 9, passband of the X3D-display based on simulated data: a) $d = 0; t = 10\%$, b) $d = 0; t = 30\%$, c) $d = 10; t = 10\%$, d) $d = 10; t = 30\%$.

4.2 Performance analysis for varying distortions

The perceived distortion values discussed in the previous section are defined in the spatial domain. Since we perform all processing in the spectral domain, we will transfer the results of that discussion to the spectral domain. For this purpose, we will assume that a distortion of t percentages in the spatial domain corresponds to t_{db} difference in decibels between the input signal and the strongest component inside the circle of interest. The relation between t and t_{db} is defined by the following well known expression:

$$t_{db} = -20\log_{10}(t/100).$$

In the case of the display under consideration, namely the X3D-display, the passband regions for two different disparities (0 and 10) and two different distortion values (10% and 30%) are given in Figure 9. This figure nicely illustrates that different filters are required for different values of distortion. Moreover, it confirms the observation from Section 3.3 that different filters are also required for different disparity levels.

Another important observation to be made here is related to the threshold of 26dB used in Sections 2.3 and 3.3. This threshold has been experimentally selected in [10] such that there are no visible (barely visible) distortions. According to the discussion in this section, 26dB corresponds to a 5% distortion. According to 5, 5% distortion is not visible. Since 26dB is also not visible (barely visible), this is an indirect proof that our assumption in this section related to transferring the results presented in 5 from spatial to spectral domain is valid.

5. ARTEFACT MITIGATION FRAMEWORK WITH SHARPNESS CONTROL

In order to visually optimize video content for a given multiview display, we propose artifact mitigation framework. It allows the user to specify the percentage of visible distortion over the original signal. The framework does the necessary processing to maintain the distortions within the selected limit, taking into account the display passband for different disparity values. It consists of two modules, shown in Figure 10 – offline processing module, where the display is measured and real-time processing module, which filters the input image according to its apparent depth and selected distortion limits. During the measurements in the offline processing module, one derives the passband of the display for a range of disparity values as explained earlier. Each passband can be approximated by a rectangle, for example as described in section 6.1 below. The output from the module is stored in two tables. One table contains the height of the equivalent passband for various disparity values and levels of distortion, and the other table – the corresponding width of the passband.

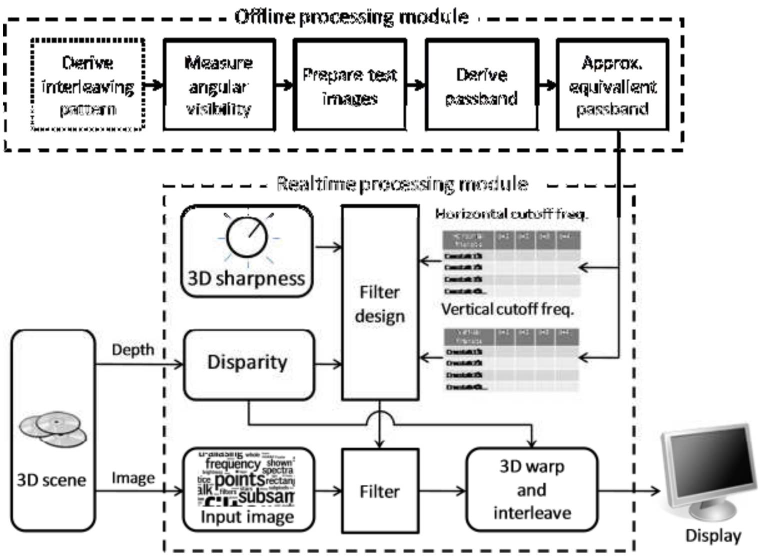

Figure 10, artifact mitigation framework.

The realtime processing module uses these two tables to design the optimal filter for the input image. We consider that the input to the framework is a 3D scene in image-plus-depth format. Other possible inputs are subtitle track or GUI widgets with known depth. The apparent depth encoded in the scene is then converted to suitable disparity value, according to the display size and resolution. The disparity value is used to select the corresponding column in each passband table. The user can set the value of the desired distortion level. We refer to this parameter as "3D-sharpness", since it controls the tradeoff between visibilities of details versus visibility of Moiré artifacts. The value of "3D-sharpness" is used to select the corresponding row of each table. The row and column selection in each table selects a cell. The values in the selected cells give the desired vertical and horizontal cutoff frequencies of an anti-aliasing filter. These cutoff frequencies are used for designing the filters. We describe one way to design such filter in Section 6.2 below. The filter is then applied on the input image before 3D warping and interleaving. Such filter mitigates the aliasing artifacts for the given disparity level and provides a desired level of "3D-sharpness".

6. DESIGN OF TUNEABLE ANTI-ALIASING FILTERS

6.1 Approximation of equivalent passband

The passband of a multiviev display for a given disparity and desired "3D-sharpness" has a nonuniform 2D shape (e.g. see Figure 9). In order to represent an image on the display properly we have to pre-filter the image with a filter having such passband as illustrated in Figure 10. In theory, we could design a 2D filter approximating the desired 2D shape. However, in practice, designing 2D filters is considerably more complicated than designing 1D filters and the implementation of a 2D filter can be computationally demanding. Therefore, in many cases, the desired 2D filter is approximated by two 1D filters, one for the horizontal direction and the other one for the vertical direction. Although, such 1D filters are just a rough approximation of the desired 2D shape, in turns out that in most cases this is good enough. For example, in our previous work 6, 7, we have shown that visually good results can be achieved by using separable 1D filters that approximate the required 2D shape. Another reason why 1D filters are good enough lies in the fact that in this paper we introduce the concept of user-tunable filters. Since the user can and will change the bandwidths of both filters according to his need, it is not too important to have 'perfect' filters.

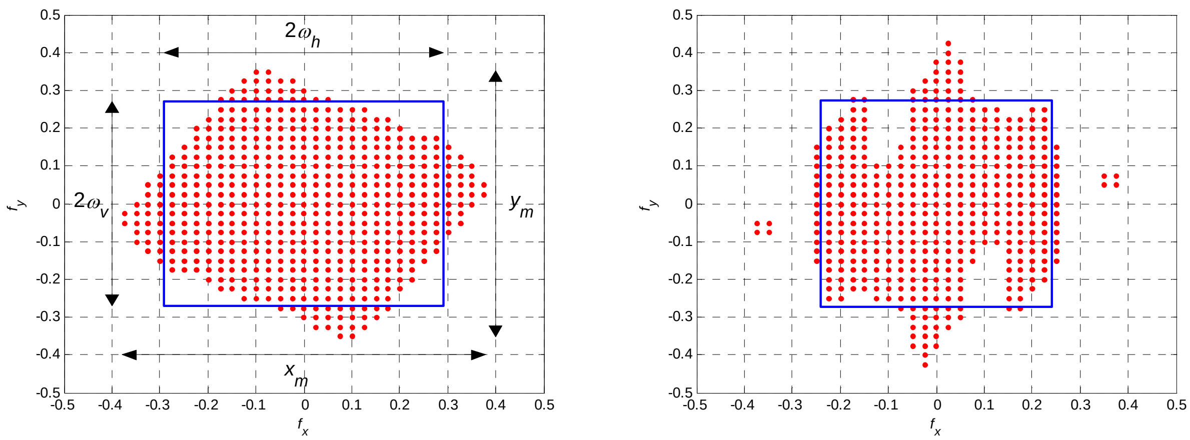

(a) (b)

Figure 11, approximating the desired passband with a rectangle: a) $d = 0; t = 5\%$, b) $d = 10; t = 30\%$.

In order to use separable 1D filters, we have to approximate the desired passband shape with a rectangle. There are many ways how an arbitrary shape can be approximated with a rectangle. In our case, we will impose following two constraints: First, we want that the area covered by the rectangle is equal in size to the original passband area, and, second, the ratio between the maximum passband value in horizontal and vertical direction should be preserved. Taking these into account, it turns out that the parameters of the rectangle can be evaluated as:

$$\omega_h = \frac{1}{2}\sqrt{\frac{x_m}{y_m}A}; \;\; \omega_v = \frac{1}{2}\sqrt{\frac{y_m}{x_m}A}\,,$$

where $2\omega_h$ and $2\omega_v$ are the width and height of the rectangle, respectively, y_m and x_m are the maximum values of the passband in horizontal and vertical direction, respectively, and A is the passband area. These parameters are illustrated in

Figure 11a. Moreover, Figure 11a {Figure 11b} shows the approximations of passband for the X3D-display for disparity 0 and 5% distortion {disparity 10 and 30% distortion}. As it can be seen, particularly in Figure 11b, approximation is not always the best one due to the weird shapes of the desired passband. Nevertheless, as we demonstrate in Section 7, our approximation is good enough in practice. Parameters, ω_h and ω_v derived in the above manner correspond to the normalized cutoff frequencies of the two separable 1D filters.

By performing the approximation for various distortion levels and disparities, we end up with a set of cutoff frequencies in horizontal and vertical direction. These frequencies can be stored in a table, in order to be used by the realtime processing module as illustrated in Figure 10. It should be pointed out that although in practice, ω_h and ω_v, are evaluated for discrete values of disparity and distortion in order to have tables of reasonable size, we can easily interpolate for missing values. Linear interpolation has turned out to be satisfactory.

6.2 Filter design

For a given disparity and distortion level, based on the desired cutoff frequencies that are derived in a manner described in the previous section, we design two 1D filters. For designing each of these filters we used the windowing technique [14]. The used window was the Kaiser window with $\beta = 2.2$. This will result in filters with the first side lobe at approximately -30dB. This attenuation has turned out to be high enough in practice (similar conclusion like for distortion can be drawn, that is, -30dB corresponds to approximately 3% distortion). The windowing technique has been selected due to its simplicity. Since the idea is to design filters in real time based on the user preference and 3D content we need a fast design method.

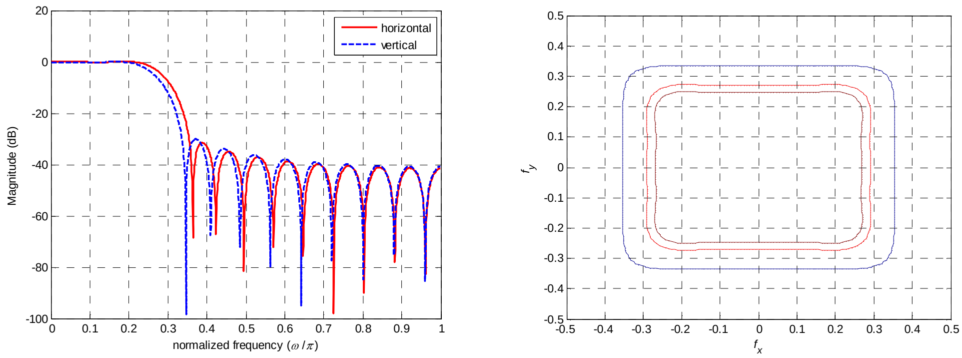

Figure 12, filters designed for the X3D-display for $d = 0; t = 5\%$: a) magnitude response of the vertical and horizontal filter, b) magnitude response of the corresponding 2D filter – contour for -3dB (innermost line), -6dB, and -30dB (outermost line).

As an example, the design of filters for the X3D-display for disparity 0 and 5% distortion is considered. The corresponding cutoff frequencies are $\omega_h = 0.291$ and $\omega_v = 0.272$. The magnitude responses of the designed 1D filters are given in Figure 12a. The magnitude (contour) of the corresponding 2D filter is given in Figure 12b. The -6dB level corresponds to the desired cutoff frequencies. The order of both filters is $N = 24$.

7. RESULTS

In Figure 13 we show the approximated X3D-display passband for several disparities between 0 and 10. Notably, the passband area does decrease monotonically with the increase of the disparity. The outer, red contours represent the passband area if distortion levels of 30% are allowed. The inner, blue contours represent the more strict, smaller passband area where distortion levels of less than 5% are desirable. One could see, that while the passbands for 30% distortion are always bigger than those for 5%, there is no visible relation between the two. Note, that for multiview displays with different interleaving pattern and visibility mask the relation between passband area and disparity of the image will most probably change.

Some examples of the effect of the designed anti-aliasing filters can be seen in Figure 14. All images on that figure are simulated output of the display as it would be seen directly from the front. The top row of images (Figure 14a-c) are rendered with zero disparity, while the bottom row (Figure 14d-f) are rendered with disparity $d = 5$. Images in the left column are simulated with no pre-filter, and the color banding and Moiré artifacts are clearly visible. Images in the center column are prefiltered with the anti-aliasing filter for $t = 30\%$ and the corresponding disparity of $d = 0$ (top) and $d = 5$ (bottom). One can see that most artifacts are mitigated, but some residual aliasing is visible. The images in the right column are pre-filtered with the anti-aliasing filter for $t = 5\%$, and exhibit even less artifacts, however at the expense of texture loss.

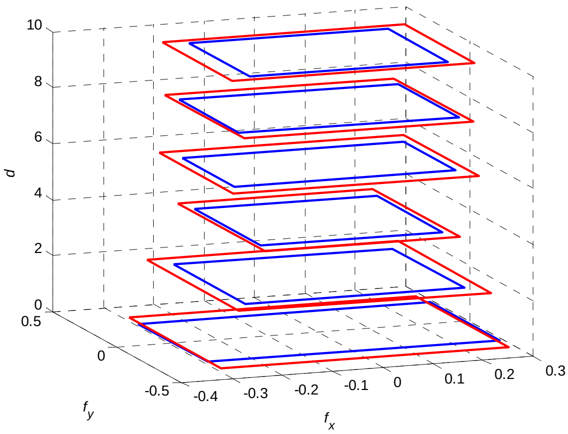

Figure 13. passband for disparities $d = 0,2,4,6,8,10$, for $t = 5\%$ (blue), and $t = 30\%$ (red).

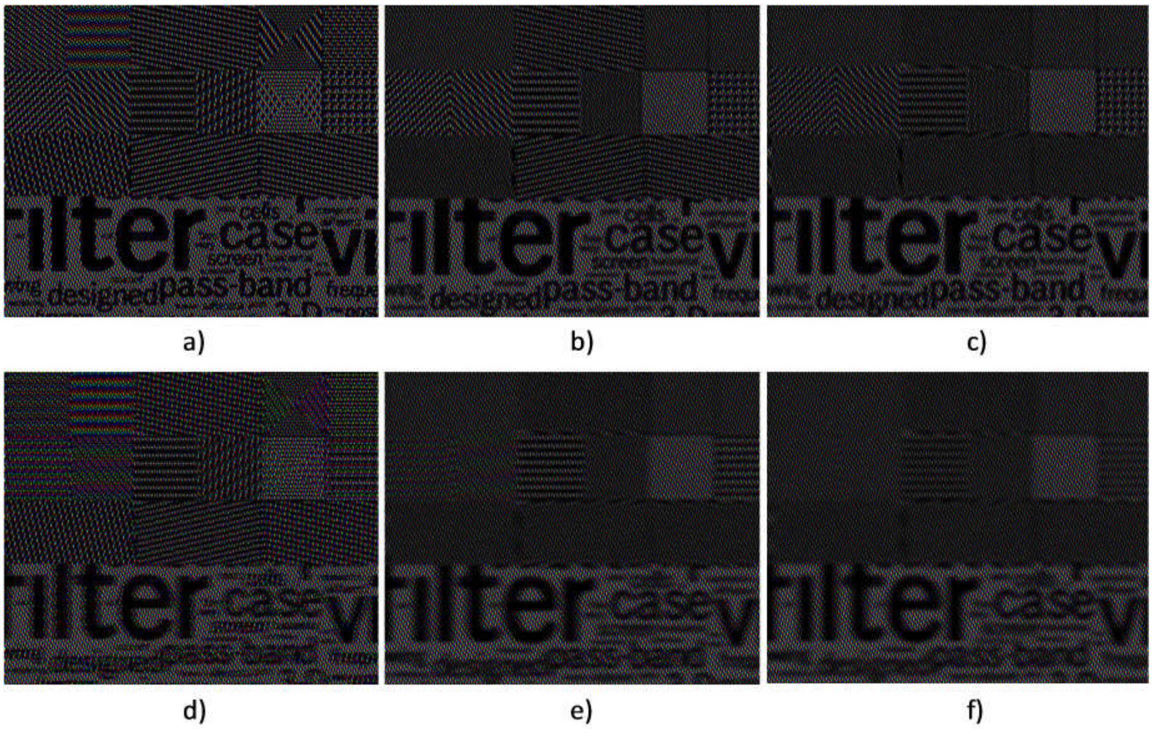

Figure 14. effect of the designed anti-aliasing filters for different disparity and distortion levels (simulated outputs): (a-c) test image with no disparity, a) without pre-filtering, b) pre-filtered with the filter for $d = 0; t = 30\%$,c) pre-filtered with the filter for $d = 0; t = 5\%$ (d-e) test image with disparity 5, d) without pre-filtering, e) prefiltered with the filter for $d = 5; t = 30\%$, f) pre-filtered with the filter for $d = 5; t = 5\%$.

8. CONCLUSIONS

We proposed a model of a multiview display which considers the display as an image processing channel. The model assumes that the input is in image-plus-depth format. We used measurement data to construct the visibility mask of the display, and used it to simulate the output of that channel. We analyzed the distortions, introduced by the channel for test images with various frequency components and disparity values. We derived multiple so-called passbands, which define combinations of frequency components and disparity values, which pass through the channel with distortions lower than the given threshold. We proposed methodology for design of tunable filters, which can be used for realtime anti-aliasing of multiview 3D images. Such tunable filters allow the user to select the desired level of “3D-sharpness” and control the trade-off between visibility of details and that of artifacts. Finally, we gave some practical results for images, filtered with anti-aliasing filters optimized for one 8-view autosterescopic display.

9. ACKNOWLEDGMENTS

The work is partially sponsored by Academy of Finland (project no. 213462, Finnish Programme for Centres of Excellence in Research 2006-2011) and Nokia Scholarship Grant provided by the Nokia Foundation.

REFERENCES

1. S. Pastoor, “3D displays”, in (Schreer, Kauff, Sikora, edts.) *3D Video Communication*, Wiley, 2005.
2. N. Dodgson, “Autostereoscopic 3D Displays,” *Computer* , vol.38, no.8, pp. 31- 36, Aug. 2005, IEEE, 2005.
3. W. IJsselsteijn, P. Seuntiens and L. Meesters, “Human factors of 3D displays”, in (Schreer, Kauff, Sikora, edts.) *3D Video Communication*, Wiley, 2005.
4. J. Konrad and P. Agniel**,** "Subsampling models and anti-alias filters for 3-D automultiscopic displays," *IEEE Trans. Image Process.*, vol. 15, pp. 128-140, Jan. 2006.
5. F.Kooi, A. Toet, “Visual comfort of binocular and 3D displays”, Displays, Volume 25, Issues 2-3, August 2004, Pages 99-108, ISSN 0141-9382, DOI: 10.1016/j.displa.2004.07.004, 2004.
6. A. Boev, R. Bregovic, A. Gotchev, “Methodology for design of anti-aliasing filters for autostereoscopic displays”, Special issue on Advanced Techniques on Multirate Signal Processing for Digital Information Processing, *Journal of IET Signal Processing*, to be published (2010).
7. A. Boev, R. Bregovic, A. Gotchev, K. Egiazarian, “Anti-aliasing filtering of 2D images for multi-view auto-stereoscopic displays”, in Proc. *of The 2009 International Workshop on Local and Non-Local Approximation in Image Processing, LNLA 2009*, Helsinki, Finland, 2009.
8. X3D-23” Users’ Manual. NewSight GmbH. Firmensitz Carl-Pulfrich-Str. 1 07745 Jena, 2006.
9. A. Nashel and H. Fuchs. “Random hole display: A non-uniform barrier autostereoscopic Display”. In proc. of *3DTV Conference: The True Vision – Capture, Transmission and Display of 3D Video*, 2009.
10. A. Boev, R. Bregovic, A. Gotchev, “Measuring and modeling per-element angular visibility in multiview displays”, Special issue on 3D displays, Journal of Society for Information Display, 2010.
11. B. Wandell, “*Foundations of Vision*”, Sinauer Associates, 1995.
12. Z. Wang, A. Bovik, H. Sheikh and E. Simoncelli, “Image quality assessment: From error visibility to structural similarity”, *IEEE Trans. Image Processing*, vol. 13, No. 4, pp. 600-612, 2004.
13. S. Winkler, “Perceptual Video Quality Metrics – A review”, in H. Wu and K. Rao, eds. “*Digital video image quality and coding*”, ch. 5, CRC press, 2006.
14. S. K. Mitra, *Digital signal processing: A computer based approach*, New York: McGrow-Hill, 2005.